The Astronomical Journal, 157:219 (5pp), 2019 June https://doi.org/10.3847/1538-3881/ab19bb

Measurement of CH_3D on Titan at Submillimeter Wavelengths

Alexander E. Thelen[1,2], Conor A. Nixon[2], Martin A. Cordiner[1,2], Steven B. Charnley[2], Patrick G. J. Irwin[3], and Zbigniew Kisiel[4]

[1] Department of Physics, Catholic University of America, 620 Michigan Avenue NE, Washington, DC 20064, USA; alexander.e.thelen@nasa.gov
[2] NASA Goddard Space Flight Center, 8800 Greenbelt Road, Greenbelt, MD 20771, USA
[3] Atmospheric, Oceanic and Planetary Physics, Clarendon Laboratory, University of Oxford, Parks Road, Oxford, OX1 3PU, UK
[4] Institute of Physics, Polish Academy of Sciences, Al. Lotnikøw 32/46, 02-668 Warszawa, Poland
Received 2019 February 15; revised 2019 March 27; accepted 2019 April 14; published 2019 May 7

Abstract

We present the first radio/submillimeter detection of monodeuterated methane (CH_3D) in Titan's atmosphere, using archival data from of the Atacama Large Millimeter/submillimeter Array (ALMA). The $J_K = 2_1-1_1$ and $J_K = 2_0-1_0$ transitions at 465.235 and 465.250 GHz (~0.644 mm) were measured at significance levels of 4.6σ and 5.7σ, respectively. These two lines were modeled using the Non-linear optimal Estimator for MultivariatE spectral analySIS (NEMESIS) radiative transfer code to determine the disk-averaged CH_3D volume mixing ratio $= 6.157 \times 10^{-6}$ in Titan's stratosphere (at altitudes >130 km). By comparison with the CH_4 vertical abundance profile measured by Cassini–Huygens mass spectrometry, the resulting value for D/H in CH_4 is $(1.033 \pm 0.081) \times 10^{-4}$. This is consistent with previous ground-based and in situ measurements from the Cassini–Huygens mission, though slightly lower than the average of the previous values. Additional CH_3D observations at higher spatial resolution will be required to determine a value truly comparable with the Cassini–Huygens CH_4 measurements, by measuring CH_3D with ALMA close to Titan's equator. In the post-Cassini era, spatially resolved observations of CH_3D with ALMA will enable the latitudinal distribution of methane to be determined, making this an important molecule for further studies.

Key words: planets and satellites: atmospheres – planets and satellites: composition – radiative transfer – submillimeter: planetary systems

1. Introduction

Methane (CH_4), one of the primary constituents of Titan's atmosphere, was first detected by Kuiper (1944) and has since been studied through myriad ground- and space-based observations. The photo- and ionic chemistry of CH_4 and Titan's most abundant atmospheric constituent, N_2, in the upper atmosphere are responsible for the large quantity of trace organic species discovered during the *Voyager-1* and Cassini eras, and are important for the formation of haze, clouds, and Titan's methane-based hydrological cycle. However, the source of Titan's atmospheric CH_4 reservoir is still unknown, as are the processes by which it may be replenished.

Titan's CH_4 volume mixing ratio was found to be 5.65×10^{-2} near the surface at the location of the Huygens landing site (~10°S) with the Gas Chromatograph Mass Spectrometer (GCMS), decreasing with altitude to the tropopause (~45 km); an average stratospheric value of 1.48×10^{-2} was measured between ~75–140 km (Niemann et al. 2010). This measurement is compatible with the initial determination of stratospheric CH_4 abundance derived from the 7.7 μm ν_4 band of CH_4 by the Cassini Composite Infrared Spectrometer (CIRS), found to be $(1.6 \pm 0.5) \times 10^{-2}$ (Flasar et al. 2005). Subsequent observations of the CH_4 ν_4 band were used to probe Titan's atmospheric temperature with CIRS throughout the Cassini mission by holding the GCMS CH_4 profile as latitudinally invariant. However, studies with the Keck II Near Infrared Spectrometer (NIRSPEC) and the Cassini Visual and Infrared Mapping Spectrometer (VIMS) suggested possible variations in Titan's atmospheric CH_4 (Penteado & Griffith 2010; Penteado et al. 2010). Through the combination of two separate CH_4 bands in focal planes 1 and 4 of Cassini/CIRS, Lellouch et al. (2014) found the CH_4 mole fraction to vary between ~1%–1.5% in the lower stratosphere at 12 locations from 70°N–80°S during Titan's northern winter (~2005–2010). This roughly symmetric distribution of CH_4 may persist throughout a Titan year (~29.5 yr), and presents important implications for photochemical and dynamical models of Titan's atmosphere.

Monodeuterated methane (CH_3D) was tentatively identified on Titan by Gillett (1975) in observations of the 8.6 μm band with the Kitt Peak National Observatory (KPNO), and confirmed by Kim & Caldwell (1982) in combination with data from the Infrared Telescope Facility (IRTF) and the *Voyager-1* Infrared Radiometer Interferometer and Spectrometer (IRIS). Later observations with these facilities (Owen et al. 1986; de Bergh et al. 1988; Coustenis et al. 1989; Orton 1992; Penteado et al. 2005), the Infrared Space Observatory (ISO; Coustenis et al. 2003), and through both components of the Cassini–Huygens mission (Bézard et al. 2007; Coustenis et al. 2007; Abbas et al. 2010; Niemann et al. 2010; Nixon et al. 2012) have further constrained Titan's atmospheric deuterium-to-hydrogen ratio (D/H). With an average value measured to be 1.36×10^{-4} during the Cassini era (see Nixon et al. 2012, and references therein), Titan is closer to Earth in terms of atmospheric deuterium enrichment than the giant planets, leading to possible constraints on the formation and sustainability of its atmosphere (Mousis et al. 2002b; Bézard et al. 2014, and references therein).

Due to the dependence on atmospheric temperature for many CH_4 observations in the infrared (IR), measurements of Titan's CH_3D abundance may provide a second method for determining possible CH_4 variations with latitude, while further constraints on Titan's D/H will help unravel the history of its formation (Mandt et al. 2009). Previous searches for CH_3D in the interstellar medium using submillimeter facilities were

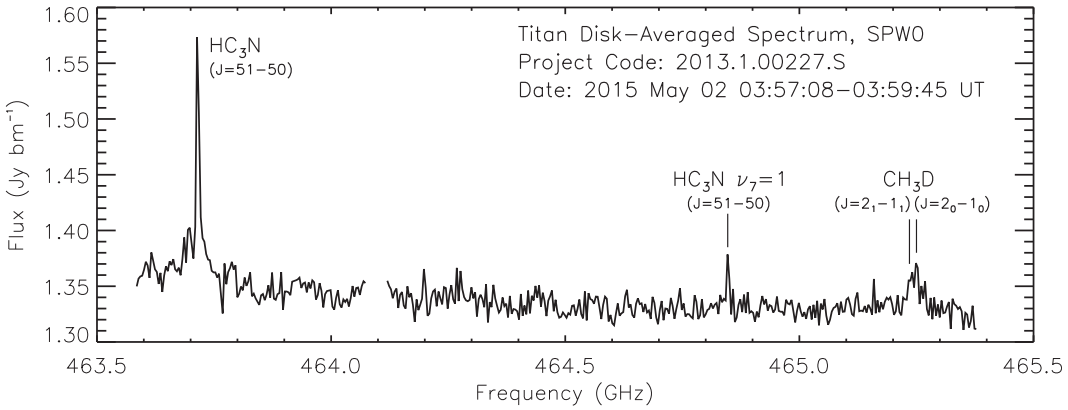

Figure 1. Complete disk-averaged spectrum of Titan from ALMA observations on 2015 May 2. The spectrum also includes two HC_3N lines ($\nu = 0$ and $\nu_7 = 1$) in addition to the two CH_3D $J = 2-1$ transitions at 465.235 and 465.250 GHz. Flux at 464.1 GHz has been flagged (removed) during the ALMA data reduction process due to terrestrial O_3 absorption.

unsuccessful (Pickett et al. 1980; Womack et al. 1996), or provided a tenuous detection of the $J = 1-0$ transition (Sakai et al. 2012). However, the advent of the Atacama Large Millimeter/submillimeter Array (ALMA) and Titan's relatively large atmospheric CH_3D content provide a new method to study this molecule with high spatial and spectral resolution from the ground. Here, we detail the first definitive detection of CH_3D at submillimeter/radio wavelengths. Though these measurements were produced from short ALMA flux calibration observations of Titan and do not utilize the full capabilities of the array, they demonstrate the means by which to study Titan's CH_4 distribution and D/H in the post-Cassini era.

2. Observations

Titan is often observed as a flux calibration object for ALMA observations, resulting in many short (~157 s) observations of the moon from 2012 onward. As of 2015, ALMA Band 8 (~385–500 GHz) has been available for use, enabling a search for the $J_K = 2_1-1_1$ and 2_0-1_0 and transitions of CH_3D at 465.235 and 465.250 GHz (~0.644 mm). The $J = 1-0$ and $J = 3-2$ transitions at 232.644 GHz (1.289 mm) and 697.690–697.781 GHz (~0.430 mm), respectively, may also be observable with ALMA in Bands 6 and 9. However, the former has a lower line strength than the $J = 2-1$ transitions, and was not detected in the data set analyzed in Thelen et al. (2018) to model the nearby CO $J = 2-1$ transition at 230.538 GHz. As of the time of writing, only two observations of Titan at frequencies covering the CH_3D $J = 3-2$ transitions were taken with the lowest frequency resolution usable with ALMA (31250 kHz), and thus the CH_3D lines were unresolved (if present). Similarly, observations containing the $J = 2-1$ frequencies use low spectral resolution settings or the Atacama Compact Array, with the exception of an observation on 2015 May 2 at UT 03:57:08, for ALMA Project Code #2013.1.00227.S (where Titan was used for flux calibration). We detected both $J = 2-1$ transitions of CH_3D at 4.6σ and 5.7σ in these data from 2015 May, shown in Figure 1. Despite the somewhat coarse spectral resolution inherent to these data (3904 kHz), we resolve both spectral lines of CH_3D, which are unresolved in additional archival data at the 15625 kHz resolution. The analogous $J = 2-1$ transitions of the ^{13}C-substituted form of CH_3D at 464.838 and 464.854 GHz (directly abutting the HC_3N $\nu_7 = 1$ line, Figure 1) were not detected in these data, despite the previous detection of this molecule in the IR (Bézard et al. 2007).

We followed the methodology described in previous works utilizing the ALMA flux calibration data of Titan (e.g., Cordiner et al. 2014; Lai et al. 2017; Thelen et al. 2018, 2019) to obtain disk-averaged spectra and calibrated image cubes. Using the Common Astronomy Software Applications (CASA) package version 5.1.2, we re-ran the ALMA data calibration scripts available with raw data from the ALMA Science Archive[5] to ensure that spectral lines in Titan's atmosphere are not flagged (such as HC_3N and CO), and to include the updated flux model for Titan (see ALMA Memo #594[6]). Imaging was completed using the `Hogbom clean` algorithm with a pixel size = 0.″1 × 0.″1 and a flux threshold of 10 mJy—roughly twice the noise level. The beam FWHM = 0.″767 × 0.″491 for this observation, which is comparable to Titan's angular size on the sky (~0.″7–1.″0, depending on distance and the inclusion of Titan's substantial atmosphere). Integrated flux maps of the CH_3D lines and both nearby HC_3N transitions are shown in Figure 2. Due to the relatively low signal-to-noise ratio (S/N) of the CH_3D and HC_3N $\nu_7 = 1$ lines in this observation and the large beam size compared to Titan's disk, these data are unsuitable for nuanced interpretation of latitudinal variations in Titan's atmosphere. Despite this, the spatial distribution of both HC_3N maps are consistent with contemporaneous data sets analyzed by Cordiner et al. (2017) and Thelen et al. (2019), and the discrepancies in flux found between $\nu = 0$ and vibrationally excited HC_3N lines discussed in Cordiner et al. (2018).

3. Radiative Transfer Modeling

We extracted a disk-averaged spectrum of Titan by defining a mask of pixels containing at least 90% of Titan's continuum flux, as in Lai et al. (2017). Using the method in previous studies (e.g., Molter et al. 2016; Thelen et al. 2018) to extract flux from within two times the ALMA point-spread function resulted in a dilution of the disk-averaged CH_3D lines in these data. The resulting spectrum is shown in Figure 1. We then converted the disk-averaged flux density into radiance units (nW cm^{-2} sr^{-1}/cm^{-1}) as described in Appendix A of Teanby et al. (2013) using 24 line-of-sight emission angles to model the flux from the full disk of Titan and the atmosphere up to 1200 km above the surface. The array of field-of-view

[5] http://almascience.nrao.edu
[6] http://library.nrao.edu/public/memos/alma/main/memo594.pdf

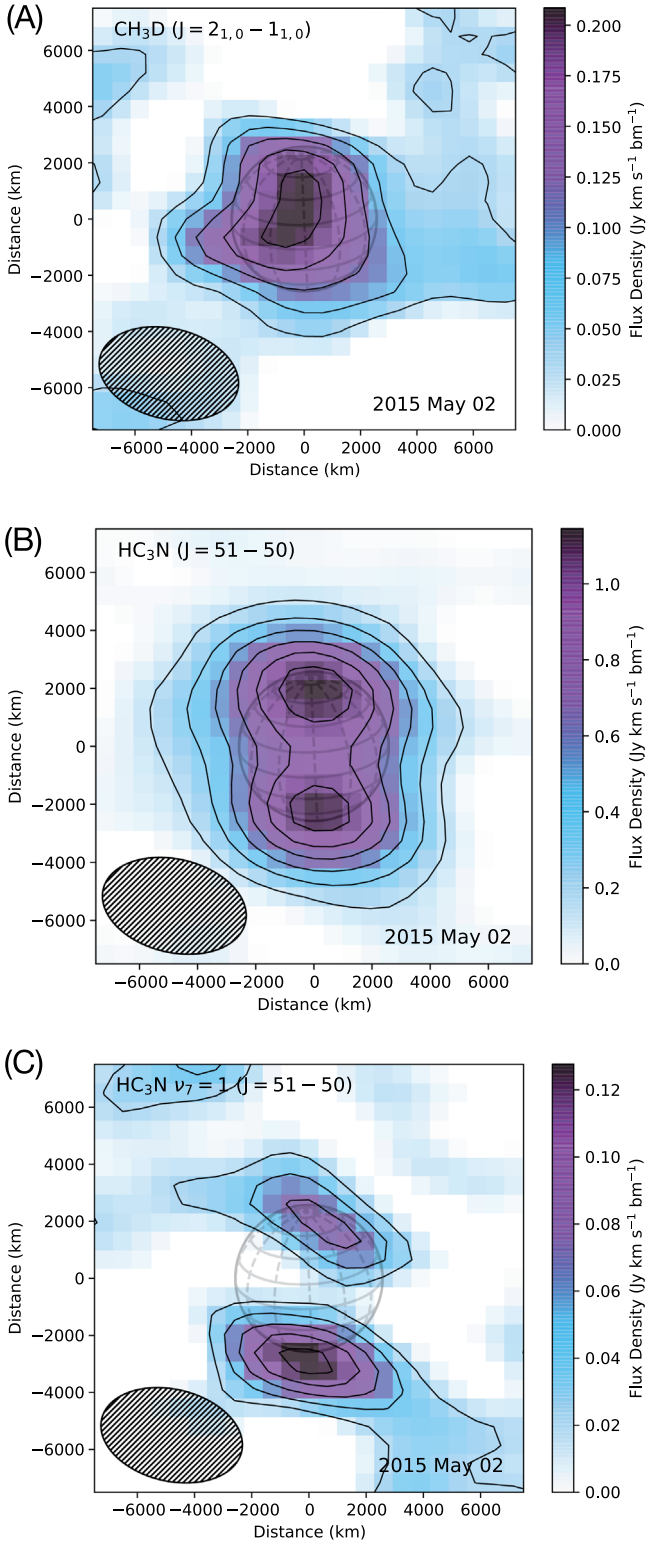

Figure 2. Integrated flux maps of the spectral lines shown in Figure 1: (A) both CH_3D transitions, (B) the ground state ($\nu = 0$) HC_3N $J = 51-50$ transition, and (C) the corresponding vibrationally excited ($\nu_7 = 1$) HC_3N transition. Contour levels are 1σ for images (A) and (C), and 3σ in image (B). The ALMA `clean` beam FWHM and orientation are shown as a hatched ellipse. Titan's surface longitude and latitude lines are shown in dashed and solid gray lines in increments of 30° and 22.°5, respectively.

averaging points increases in density toward the limb of Titan to account for limb brightening, similar to previous disk-averaged models of Titan's atmosphere in the submillimeter

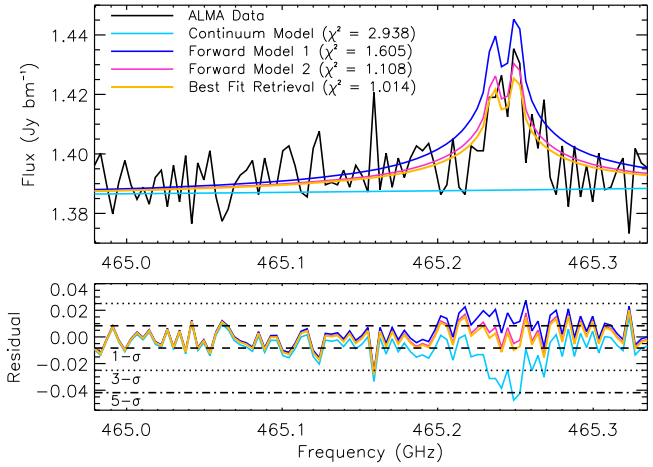

Figure 3. Top: disk-averaged ALMA data (black) with NEMESIS radiative transfer models of: Titan's continuum (teal); CH_3D spectra corresponding to the D/H ratios found by Nixon et al. (2012) and Coustenis et al. (2007; blue and magenta, respectively); and the best-fit spectrum found by scaling the a priori CH_3D profiles by NEMESIS (gold). Discrepancies between the flux scale here and in Figure 1 are due to the implementation of a scaling factor during modeling. The spectral feature at ∼465.16 GHz appears to be a noise spike, as it does not correspond to any other minor species used in our models of Titan's atmosphere. Bottom: residual spectra (model−data) for the models in the top panel. ±1, 3, and 5σ thresholds are shown in dashed, dotted, and dashed–dotted lines, respectively.

(Teanby et al. 2013; Thelen et al. 2018). Although additional emission angles may be required to accurately model higher spatial resolution data (e.g., Thelen et al. 2019), summing over 24 annuli was sufficient to model the disk-averaged radiance from these data. Radiances were converted using Titan's distance of 9.038 au. The sub-observer latitude was 24.°55 and the Doppler shift was -7.5 km s^{-1}; these values were obtained from the JPL Horizons ephemerides generator.[7] We then generated initial radiative transfer models using the Non-linear optimal Estimator for MultivariatE spectral analySIS (NEMESIS) software package (Irwin et al. 2008) to determine any offsets in the continuum level.

Titan's continuum was modeled using collisionally induced absorption from CH_4, H_2, and N_2 pairs (including isotopes), with coefficients from Borysow & Frommhold (1986a, 1986b, 1986c, 1987), Borysow (1991), and Borysow & Tang (1993). As Titan's continuum in the submillimeter is largely dependent on the tropopause temperature, we constructed a disk-averaged temperature profile using contemporaneous ALMA measurements from Thelen et al. (2018) in the stratosphere and above, and an interpolation of tropospheric temperatures found using data from the Huygens Atmospheric Structure Instrument (Fulchignoni et al. 2005) and those obtained through Cassini radio occultations (Schinder et al. 2012). This resulted in a small (<5% of the initial radiance), constant offset between the data and model, rectified by multiplying the data by a factor of 1.047. This scaling factor is consistent with previous studies using ALMA flux calibration data (see Thelen et al. 2019, and references therein), and is due to minor discrepancies between our Titan model and the one used in the CASA reduction package for ALMA data (discussed further in Thelen et al. 2018).

To obtain an accurate radiative transfer model of the CH_3D lines emitted in Titan's atmosphere, we ran NEMESIS in the line-by-line mode over a small spectral range, shown in

[7] https://ssd.jpl.nasa.gov/horizons.cgi

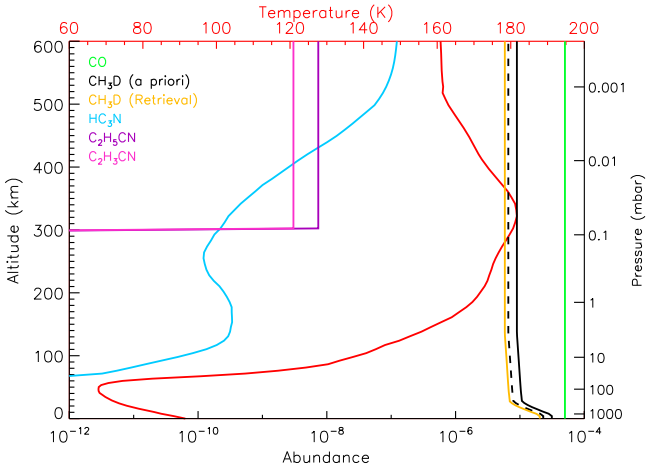

Figure 4. Atmosphere profiles used in our NEMESIS radiative transfer model: CO (green); HC_3N (teal, from Thelen et al. 2019); C_2H_3CN and C_2H_5CN (pink and purple, respectively) from Lai et al. (2017); and temperature (red) from Thelen et al. (2018). The CH_3D profiles used as a priori inputs are shown in black, corresponding to the D/H ratios from Nixon et al. (2012; solid line) and Coustenis et al. (2007; dashed line). Our best-fit model is shown in gold, corresponding to a $D/H = 1.033 \times 10^{-4}$.

Figure 3. CH_3D spectral line and partition function parameters were obtained from the Cologne Database for Molecular Spectroscopy (Womack et al. 1996; Müller et al. 2001; Bray et al. 2017). Line broadening and temperature dependence coefficients were obtained from the HITRAN 2012 database (Rothman et al. 2013). Our NEMESIS model also consists of nearby species that may influence the CH_3D line shape and nearby continuum, and an appropriate temperature-pressure profile for Titan during northern summer. We thus include N_2 and CH_4 vertical abundance profiles from Niemann et al. (2010) and Teanby et al. (2013); CO with a constant volume mixing ratio of 50 ppm (see Serigano et al. 2016, and references therein); and HC_3N, using the 2015 disk-averaged abundance profile found in Thelen et al. (2019). Though nearby emission lines of C_2H_3CN and C_2H_5CN do not strongly affect the line shape of the CH_3D lines and are undetected in the modeled spectral range of these data, these species were included for completeness using abundance profiles from Lai et al. (2017). The vertical temperature and abundance profiles included in our model are shown in Figure 4.

Due to the somewhat coarse spectral resolution settings of this observation and the relatively low S/N of both CH_3D lines (compared to the nearby HC_3N line, for example), we opted to find a best-fit spectrum using a simple scaling model (i.e., a constant multiplicative factor) of an a priori CH_3D profile. All other modeling parameters, primarily the temperature and additional gas abundance profiles, were held constant, and the CH_3D profile was set to retain the initial shape of the a priori input (that is, NEMESIS did not retrieve a continuous vertical profile). Our initial CH_3D profiles were found by multiplying in situ CH_4 data obtained with the Huygens probe (Niemann et al. 2010) by various D/H ratios. These include measurements made during the Cassini era from previous ground-based studies (Penteado et al. 2005; de Bergh et al. 2012), the Huygens GCMS (Niemann et al. 2010), and with Cassini/CIRS (Bézard et al. 2007; Coustenis et al. 2007; Abbas et al. 2010; Nixon et al. 2012), and cover a range of D/H ratios from $(1.13–1.59) \times 10^{-4}$. Spectral models using the D/H ratios $= 1.17 \times 10^{-4}$ and 1.59×10^{-4} from Coustenis et al. (2007) and Nixon et al. (2012), respectively, are shown in Figure 3 (magenta and blue spectra); the corresponding CH_3D abundance profiles are shown in Figure 4 (black lines). Models using all a priori abundance profiles converge on a single best-fit spectrum shown in Figure 3 (gold), with scaling factors producing a common CH_3D profile shown in Figure 4 (gold line). Our retrievals were most sensitive between ~100–200 km, where we find the CH_3D abundance to decrease from $(6.455–6.157) \times 10^{-6}$.

4. Discussion and Conclusions

Using archival ALMA flux calibration data of Titan from 2015, we have produced the first definitive detection of CH_3D in the submillimeter. While integrated flux maps of the ground ($\nu = 0$) and vibrationally excited ($\nu_7 = 1$) HC_3N transitions produced from the same image cube (Figures 2(B), (C)) show spatial distributions consistent with previous studies of Titan with ALMA (Cordiner et al. 2017, 2018; Thelen et al. 2019), the integrated flux map of CH_3D (Figure 2(A)) shows a lack of significant variation between the poles (less than ~30%). Though this is consistent with a constant CH_3D profile (and that of its parent molecule, CH_4) with latitude, the low spatial resolution and S/N of the CH_3D lines prohibit the interpretation of possible latitudinal variations seen in the higher resolution data acquired with Cassini/VIMS and CIRS (Penteado et al. 2010; Lellouch et al. 2014). We thus measured the disk-averaged abundance of CH_3D using the NEMESIS radiative transfer code to be a constant value $= 6.157 \times 10^{-6}$ above ~130 km, where our measurements are most sensitive. When taken with the CH_4 profile found by the Huygens GCMS (Niemann et al. 2010), our CH_3D abundance yields a $D/H = (1.033 \pm 0.081) \times 10^{-4}$.

The D/H ratio found above is within the errors of previous measurements from ISO, IRTF, KPNO, and the Cassini–Huygens mission (Coustenis et al. 2003, 2007; Penteado et al. 2005; Niemann et al. 2010; de Bergh et al. 2012), though generally lower than the average of measurements made during the Cassini era (1.36×10^{-4}; Nixon et al. 2012) and from *Voyager-1* (1.5×10^{-4}; Coustenis et al. 1989). The addition of our measurement results in a new weighted mean, $D/H = (1.203^{+0.057}_{-0.054}) \times 10^{-4}$, for observations made during the Cassini/Huygens mission, or utilizing GCMS results. The error bars on our measurement are relative, and only reflect the retrieval errors of our best-fit synthetic CH_3D spectrum. As we cannot simultaneously detect CH_4 with ALMA, any D/H measurements rely on previous data obtained in the IR by ISO, *Voyager-1,* Cassini, various ground-based facilities, or in situ data from the Huygens probe. As the GCMS abundance profile of CH_4 was determined at the probe's landing site (~10°S), disk-averaged measurements of Titan with ALMA may not yield a completely comparable D/H to previous, self-consistent measurements with the Cassini–Huygens mission. As shown during the *Voyager-1* mission and with the ISO (Coustenis et al. 1989, 2003), the measurement of Titan's D/H ratio is often not straightforward without a well-constrained measurement of CH_4. These early results were determined using CH4 abundances = 1.8%–1.9%, which would significantly lower our D/H measurement ($\sim 8.1 \times 10^{-5}$) if used instead of the Huygens/GCMS results. Further, as there is only one data set on the ALMA archive (at the time of writing) with the spectral settings and resolution capable of resolving both $J = 2–1$ transitions of CH_3D, we were unable to stack measurement sets to produce a higher S/N detection.

As such, the D/H value we report should be taken with caution, as there are many potential sources of error that are difficult to quantify in relatively low spatial resolution ALMA data—including variations in temperature and CH_4 abundance with latitude. However, despite our relatively low disk-averaged value of D/H compared to Cassini–Huygens measurements, it remains larger than the D/H values derived from CH_4 abundances for Jupiter (2.2×10^{-5}, Lellouch et al. 2001) and Saturn (1.6×10^{-5}, Fletcher et al. 2009) by almost an order of magnitude and is more in line with terrestrial D/H measurements in Earth's oceans (D/H for Vienna Standard Mean Ocean Water is $\sim 1.56 \times 10^{-4}$; see, e.g., Alexander et al. 2012). Thus, our measurement is consistent with previous observations and models that indicate Titan's CH_4 reservoir did not evolve from a Saturnian D/H value (e.g., through photochemistry or serpentinization reactions within Titan's interior; Cordier et al. 2008; Mousis et al. 2009). Instead, Titan was possibly formed from an aggregate of planetesimals that were initially enriched in deuterium from interstellar CH_4. The isotopic exchange between infalling gas phase CH_4 and H_2 in the solar nebula eventually resulted in an enhanced D/H value, which was then preserved as CH_4 condensed or was trapped within water–ice clathrates in the Saturnian subnebula (Mousis et al. 2002a, 2002b). Titan's D/H value was then modified through photochemistry, diffusion, atmospheric escape, and the outgassing of CH_4 from the interior (Cordier et al. 2008; Mandt et al. 2009), finally resulting in near an order of magnitude greater deuterium enrichment compared to Saturn as we find here.

Despite the uncertainties of our D/H measurement, the detection of CH_3D in the submillimeter allows for independent observations of the spatial variation in atmospheric CH_4 without the large dependence on simultaneous temperature measurements (as are required in many IR observations). As noted above, the lack of ALMA flux calibration observations covering the $J = 2-1$ and the adjacent transitions of CH_3D presents a need for a targeted study of Titan with longer integration times and adequate spectral resolution. With ALMA's high spatial resolution capabilities, further studies of CH_3D may enable mapping of CH_4 down to 100's of kilometers allowing for a follow-up to the study by Lellouch et al. (2014); higher S/N data will also result in CH_3D abundance measurements from a larger range of altitudes. Finally, measuring Titan's CH_3D abundance near the equator allows for a more constrained D/H when determined using data from the Huygens probe.

A.E.T. and M.A.C. were funded by the National Science Foundation Grant #AST-1616306. C.A.N. and M.A.C. received funding from NASA's Solar System Observations Program. C.A.N. was supported by the NASA Astrobiology Institute. P.G.J.I. acknowledges the support of the UK Science and Technology Facilities Council.

This paper makes use of the following ALMA data: ADS/JAO.ALMA#2013.1.00227.S, 2013.1.01010.S, and 2012.1.00688.S. ALMA is a partnership of ESO (representing its member states), NSF (USA) and NINS (Japan), together with NRC (Canada) and NSC and ASIAA (Taiwan) and KASI (Republic of Korea), in cooperation with the Republic of Chile. The Joint ALMA Observatory is operated by ESO, AUI/NRAO, and NAOJ. The National Radio Astronomy Observatory is a facility of the National Science Foundation operated under cooperative agreement by Associated Universities, Inc.

ORCID iDs

Alexander E. Thelen https://orcid.org/0000-0002-8178-1042
Conor A. Nixon https://orcid.org/0000-0001-9540-9121
Martin A. Cordiner https://orcid.org/0000-0001-8233-2436
Patrick G. J. Irwin https://orcid.org/0000-0002-6772-384X
Zbigniew Kisiel https://orcid.org/0000-0002-2570-3154

References

Abbas, M., Kandadi, H., LeClair, A., et al. 2010, ApJ, 708, 342
Alexander, C. M. O., Bowden, R., Fogel, M. L., et al. 2012, Sci, 337, 721
Bézard, B., Nixon, C. A., Kleiner, I., & Jennings, D. E. 2007, Icar, 191, 397
Bézard, B., Yelle, R., & Nixon, C. A. 2014, The Composition of Titan's Atmosphere (Cambridge: Cambridge Univ. Press)
Borysow, A. 1991, Icar, 92, 273
Borysow, A., & Frommhold, L. 1986a, ApJ, 311, 1043
Borysow, A., & Frommhold, L. 1986b, ApJ, 303, 495
Borysow, A., & Frommhold, L. 1986c, ApJ, 304, 849
Borysow, A., & Frommhold, L. 1987, ApJ, 318, 940
Borysow, A., & Tang, C. 1993, Icar, 105, 175
Bray, C., Cuisset, A., Hindle, F., et al. 2017, JQSRT, 189, 198
Cordier, D., Mousis, O., Lunine, J. I., Moudens, A., & Vuitton, V. 2008, ApJL, 689, L61
Cordiner, M. A., Lai, J. C., Nixon, C. A., et al. 2017, in IAU Symp. 13, Astrochemistry VII: Through the Cosmos from Galaxies to Planets, ed. M. Cunningham, T. Millar, & Y. Aikawa (Cambridge: Cambridge Univ. Press), 95
Cordiner, M. A., Nixon, C. A., Charnley, S. B., et al. 2018, ApJ, 859, L15
Cordiner, M. A., Nixon, C. A., Teanby, N. A., et al. 2014, ApJL, 795, L30
Coustenis, A., Achterberg, R. K., Conrath, B. J., et al. 2007, Icar, 189, 35
Coustenis, A., Bézard, B., & Gautier, D. 1989, Icar, 82, 67
Coustenis, A., Salama, A., Schulz, B., et al. 2003, Icar, 161, 383
de Bergh, C., Courtin, R., Bézard, B., et al. 2012, P&SS, 61, 85
de Bergh, C., Lutz, B., Owen, T., & Chauville, J. 1988, ApJ, 329, 951
Flasar, F. M., Achterberg, R. K., Conrath, B. J., et al. 2005, Sci, 308, 975
Fletcher, L. N., Orton, G. S., Teanby, N. A., Irwin, P. G. J., & Bjoraker, G. L. 2009, Icar, 199, 351
Fulchignoni, M., Ferri, F., Angrilli, F., et al. 2005, Natur, 438, 785
Gillett, F. C. 1975, ApJL, 201, L41
Irwin, P. G. J., Teanby, N. A., de Kok, R., et al. 2008, JQSRT, 109, 1136
Kim, S. J., & Caldwell, J. 1982, Icar, 52, 473
Kuiper, G. P. 1944, ApJ, 100, 378
Lai, J. C.-Y., Cordiner, M. A., Nixon, C. A., et al. 2017, AJ, 154, 206
Lellouch, E., Bézard, B., Flasar, F. M., et al. 2014, Icar, 231, 323
Lellouch, E., Bézard, B., Fouchet, T., et al. 2001, A&A, 370, 610
Mandt, K. E., Waite, J. H., Lewis, W., et al. 2009, P&SS, 57, 1917
Molter, E. M., Nixon, C. A., Cordiner, M. A., et al. 2016, AJ, 152, 1
Mousis, O., Gautier, D., & Bockelée-Morvan, D. 2002a, Icar, 156, 162
Mousis, O., Gautier, D., & Coustenis, A. 2002b, Icar, 159, 156
Mousis, O., Lunine, J. I., Pasek, M., et al. 2009, Icar, 204, 749
Müller, H. S. P., Thorwirth, S., Roth, D. A., & Winnewisser, G. 2001, A&A, 370, L49
Niemann, H. B., Atreya, S. K., Demick, J. E., et al. 2010, JGRE, 115, E12006
Nixon, C. A., Temelso, B., Vinatier, S., et al. 2012, ApJ, 749, 159
Orton, G. 1992, in ESA Special Pub. 338, Symp. on Titan, ed. B. Kaldeich (Noordwijk: ESA), 81
Owen, T., Lutz, B. L., & de Bergh, C. 1986, Natur, 320, 244
Penteado, P., Griffith, C., Greathouse, T., & de Bergh, C. 2005, ApJL, 629, L53
Penteado, P. F., & Griffith, C. A. 2010, Icar, 206, 345
Penteado, P. F., Griffith, C. A., Tomasko, M. G., et al. 2010, Icar, 206, 352
Pickett, H. M., Cohen, E. A., & Phillips, T. G. 1980, ApJL, 236, L43
Rothman, L. S., Gordon, I. E., Babikov, Y., et al. 2013, JQSRT, 130, 4
Sakai, N., Shirley, Y. L., Sakai, T., et al. 2012, ApJL, 758, L4
Schinder, P. J., Flasar, F. M., Marouf, E. A., et al. 2012, Icar, 221, 1020
Serigano, J., Nixon, C. A., Cordiner, M. A., et al. 2016, ApJL, 821, L8
Teanby, N. A., Irwin, P. G. J., Nixon, C. A., et al. 2013, P&SS, 75, 136
Thelen, A. E., Nixon, C. A., Chanover, N. J., et al. 2018, Icar, 307, 380
Thelen, A. E., Nixon, C. A., Chanover, N. J., et al. 2019, Icar, 319, 417
Womack, M., Apponi, A. J., & Ziurys, L. M. 1996, ApJ, 461, 897